

Transition from Hydrogen Atom to Hydride Abstraction by $\text{Mn}_4\text{O}_4(\text{O}_2\text{PPh}_2)_6$ versus $[\text{Mn}_4\text{O}_4(\text{O}_2\text{PPh}_2)_6]^+$: O–H Bond Dissociation Energies and the Formation of $\text{Mn}_4\text{O}_3(\text{OH})(\text{O}_2\text{PPh}_2)_6$

Thomas G. Carrell, Emilie Bourles, Matthew Lin, and G. Charles Dismukes*

Department of Chemistry and Princeton Environmental Institute, Princeton University,
Princeton, New Jersey 08544

Received August 26, 2002

Synthesis, characterization, and reactions of the novel manganese–oxo cubane complex $[\text{Mn}_4\text{O}_4(\text{O}_2\text{PPh}_2)_6](\text{ClO}_4)$, $1^+(\text{ClO}_4^-)$, are described. Cation 1^+ is composed of the $[\text{Mn}_4\text{O}_4]^{7+}$ core surrounded by six bidentate phosphinate ligands. The proton-coupled electron transfer (pcet) reactions of phenothiazine (pzH), the cation radical $(\text{pzH}^+)(\text{ClO}_4^-)$, and the neutral pz^\bullet radical with 1^+ are reported and compared to $\text{Mn}_4\text{O}_4(\text{O}_2\text{PPh}_2)_6$ (**1**). Compound $1^+(\text{ClO}_4^-)$ reacts with excess pzH via four sequential reduction steps that transfer a total of five electrons and four protons to 1^+ . This reaction forms the doubly dehydrated manganese cluster $\text{Mn}_4\text{O}_2(\text{O}_2\text{PPh}_2)_6$ (**2**) and two water molecules derived from the corner oxygen atoms. The first pcet step forms the novel complex $\text{Mn}_4\text{O}_3(\text{OH})(\text{O}_2\text{PPh}_2)_6$ (**1H**) and 1 equiv of the pz^+ cation by net hydride transfer from pzH. Spectroscopic characterization of isolated **1H** is reported. Reduction of **1** by pzH or a series of para-substituted phenols also produces **1H** via net H atom transfer. A lower limit to the homolytic bond dissociation energy (BDE) ($\text{1H} \rightarrow \text{1} + \text{H}$) was estimated to be >94 kcal/mol using solution phase BDEs for pzH and para-substituted phenols. The heterolytic BDE was estimated for the hydride transfer reaction $\text{1H} \rightarrow \text{1}^+ + \text{H}^-$ (BDE ~ 127 kcal/mol). These comparisons reveal the O–H bond in **1H** to be among the strongest of any Mn–hydroxo complex measured thus far. In three successive H atom transfer steps, **1H** abstracts three hydrogen atoms from three pzH molecules to form complex **2**. Complex **2** is shown to be identical to the “pinned butterfly” cluster produced by the reaction of **1** with pzH (Ruettinger, W. F.; Dismukes, G. C. *Inorg. Chem.* **2000**, *39*, 1021–1027). The Mn oxidation states in **2** are formally $\text{Mn}_4(2\text{II}, 2\text{III})$, and no further reduction occurs in excess pzH. By contrast, outer-sphere electron-only reductants such as cobaltacene reduce both 1^+ and **1** to the all Mn(II) oxidation level and cause cluster fragmentation. The reaction of pzH^{++} with 1^+ produces **1H** and the pz^+ cation by net hydrogen atom transfer, and terminates at 1 equiv of pzH^{++} with no further reaction at excess. By contrast, pz^\bullet does not react with 1^+ at all, indicating that reduction of 1^+ by electron transfer to form pz^+ does not occur without a proton (pcet to 1^+ is thermodynamically required). Experimental free energy changes are shown to account for these pcet reactions and the absence of electron transfer for any of the phenothiazine series. Hydrogen atom abstraction from substrates by **1** versus hydride abstraction by 1^+ illustrates the transition to two-electron one-proton pcet chemistry in the $[\text{Mn}_4\text{O}_4]^{7+}$ core that is understood on the basis of free energy consideration. This transition provides a concrete example of the predicted lowest-energy pathway for the oxidation of two water molecules to H_2O_2 as an intermediate within the photosynthetic water-oxidizing enzyme (vs sequential one-electron/proton steps). The implications for the mechanism of photosynthetic water splitting are discussed.

Introduction

Oxidation/reduction reactions are the primary source for energy transduction processes in biology. Mechanistically,

these reactions can be concerted or go via distinct electron/proton pathways having markedly different coupling strength between the electron and proton coordinates, thus giving rise to a rich diversity of reaction types denoted collectively as proton-coupled electron transfer (pcet) reactions.^{1–4} From a thermodynamic standpoint, pcet lowers the required driving

* To whom correspondence should be addressed. E-mail: dismukes@princeton.edu.

force relative to the two processes performed separately and thus offers a favorable mechanism for lowering kinetic barriers to endo- and isothermic reactions.^{5,6}

A biological example is found in the four-electron/four-proton oxidation of H₂O to O₂ during photosynthesis. This process occurs at an inorganic cluster composed of Mn₄O_x-Ca₁Cl_y known as the water oxidizing complex (WOC) bound within the photosystem II protein complex (PSII). The PSII-WOC cycles through five oxidation states during catalysis, each involving the removal of one electron via an essential tyrosyl radical, and in some steps, zero or more protons are released into solution. The energetics of this system have inspired proposals postulating direct hydrogen atom transfer to tyrosyl radical as a required feature of water oxidation.^{7–11} For example, the estimated O–H bond dissociation energy (BDE_{OH}) of 86 kcal/mol for tyrosine dictates that the tyrosyl radical is not energetically capable of cleaving the O–H bond in water (119 kcal/mol) without stabilization of the resulting hydroxyl radical product by delocalization with the Mn cluster. Support has come from model complexes that show it is energetically more favorable to cleave the O–H bond from a water or hydroxide ligand bound in a series of Mn^{III} and Mn^{IV} complexes.^{10,12–14}

As a test of these concepts, we previously described pcut reactions of Mn₄O₄(O₂PPh₂)₆ (**1**), which contains the Mn₄O₄⁶⁺ “cubane” core surrounded by six diphenylphosphinate chelates. The reduction of **1**, either electrochemically or by the addition of strong reductants such as CoCp₂, results in irreversible cluster decomposition by reduction to monomeric Mn^{II}.¹⁵ However, coupling the electron and proton transfer steps by using a suitable hydrogen atom donor such as phenothiazine (pzH) leads to sequential transfer of four H atoms, terminating in the reduced cluster Mn₄O₂(O₂PPh₂)₆ (**2**) and two water molecules.¹⁶ Compound **2** contains the Mn₄O₂⁶⁺ “butterfly” core in oxidation state Mn₄(2II, 2III). Herein, we extend this study to illustrate the transition to metal-centered hydride transfer chemistry involving the one-electron oxidized cluster [Mn₄O₄(O₂PPh₂)₆]ClO₄, **1**⁺(ClO₄⁻).

We also illustrate the range of pcut reactions that occur between **1**⁺ and pzH, the pzH⁺ radical cation, and the neutral pz• radical. The O–H bond dissociation energies for both **1** and **1**⁺ are compared and discussed in relation to water oxidation proposals for PSII-WOC.

Experimental Section

Materials. All solvents were purchased from EM Science and were spectrophotometric grade. Deuterated solvents for NMR were purchased from Cambridge Isotopes. HClO₄ (70% solution in H₂O) was purchased from Fisher Scientific. Phenothiazine, HOTf (OTf⁻ = trifluoromethanesulfonate, CF₃SO₃⁻), and (Me₃Si)OTf were purchased from Aldrich. Mn₄O₄(O₂PPh₂)₆ (**1**) was prepared as described elsewhere.¹⁷

Instrumentation. UV–vis spectra were measured on an HP-8452A diode array spectrophotometer using quartz cuvettes with a 1.0 cm path length. ¹H NMR spectra were obtained on either a Varian Mercury-300 or INOVA-400 MHz spectrometer. FTIR spectra were measured on a Nicolet 730 FTIR spectrometer, using KBr pellets for solid samples or a liquid IR cell with KBr plates and a 0.2 mm path length for solution samples. Electrospray ionization (ESI) mass spectra were recorded on a Hewlett-Packard HP5989B spectrometer with a capillary voltage of 80 V. Sample concentrations in the range 0.1–1 mM were used. EPR spectra were recorded at 9.5 GHz on a Bruker ESP300 spectrometer equipped with Oxford cryostat model 900.

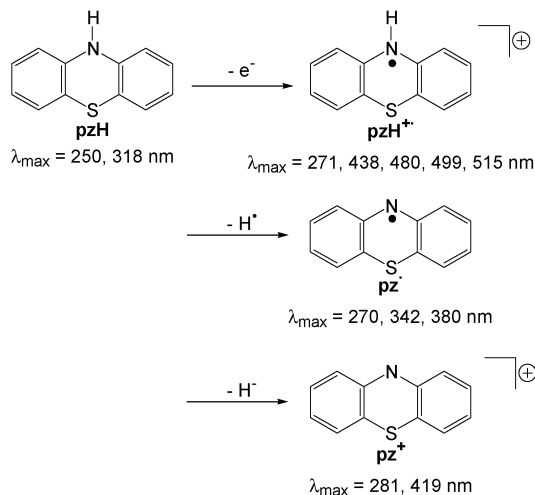
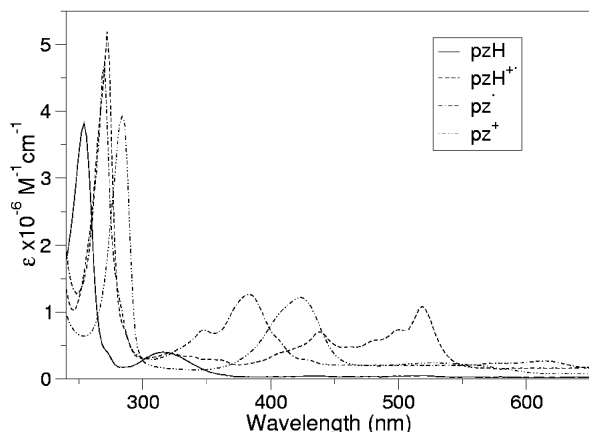
Absorbance Titrations. pzH (5.0 mM solution in CH₂Cl₂) was added in 0.25 equiv increments to 2.0 mL of a 0.025 mM solution of **1**⁺(ClO₄⁻) in CH₂Cl₂. All spectral changes were complete within seconds of mixing. The absorbance spectrum of the solution (190–820 nm, 20–25 °C) was recorded following each addition of pzH.

Synthesis of [Mn₄O₄(O₂PPh₂)₆]ClO₄, **1⁺(ClO₄⁻).** Compound **1** (70 mg, 4.4 × 10⁻⁵ mol) was suspended in 25 mL of CH₂Cl₂. HClO₄ (3 equiv, 1.32 × 10⁻⁴ mol, 1.32 mL of 0.10 M solution in CH₃CN) was added dropwise to this air-saturated suspension, forming a clear dark red-brown solution. The solvent was removed in vacuo, and the residue was then extracted by a small quantity of CH₂Cl₂. This solution was filtered over Celite to remove any particulate matter, and the solvent was evaporated using a stream of air. Final yield 70%. Purity was assessed spectroscopically as described in the Results section. Freshly synthesized solutions of **1**⁺(ClO₄⁻) are not stable over the course of many hours, a feature that is due to the presence of residual water introduced by the perchloric acid. However, the isolated microcrystalline solid is stable after drying under vacuum and is stored in the absence of water.

Synthesis of Mn₄O₃(OH)(O₂PPh₂)₆, **1H.** Synthesis of **1H** was performed by reaction of **1**⁺(ClO₄⁻) with 1 equiv of pzH. Absorbance measurements during the reaction show clean isosbestic behavior (λ_i = 300 and 400 nm) and stoichiometric conversion of pzH to the pz⁺ cation based on the known molar absorptivities (λ_{max} = 280 and 422 nm). Purple crystals of pz⁺(ClO₄⁻) precipitate from this solution over a two-day period. Absorbance measurements showed that the remaining solution did not contain a trace of pzH or its oxidized products (Supporting Information). This crystalline solid exhibits UV–vis, FTIR, and NMR spectra that are identical to those of the pz⁺ cation prepared by deprotonation of pzH using Et₃N. The separation of pz⁺(ClO₄⁻) from **1H** was also achieved by stripping the solvent from the reaction mixture in vacuo to dryness immediately following the addition of 1 equiv of pzH to **1**⁺(ClO₄⁻), followed by extraction with either CH₂Cl₂ or CHCl₃.

- (1) Holm, R.; Donahue, J. P. *Polyhedron* **1993**, *12*, 571–589.
- (2) Holm, R. H. *Chem. Rev.* **1987**, *87*, 1401–1449.
- (3) Mayer, J. M. *Acc. Chem. Res.* **1998**, *31*, 441–450.
- (4) Roth, J. P.; Yoder, J. C.; Won, T.-J.; Mayer, J. M. *Science* **2001**, *294*, 2524–2526.
- (5) Hammes-Schiffer, S. *ChemPhysChem* **2002**, *3*, 33–42.
- (6) Cukier, R. I.; Nocera, D. G. *Annu. Rev. Phys. Chem.* **1998**, *49*, 337–369.
- (7) Gilchrist, M. L.; Ball, J. A.; Randall, D. W.; Britt, D. *Proc. Natl. Acad. Sci. U.S.A.* **1995**, *92*, 9545–9549.
- (8) Hoganson, C. W.; Lydakis-Simantiris, X.; Tang, X.-S.; Tommos, C.; Warnecke, K.; T., B. G.; Diner, B. A.; McCracken, J.; Styring, S. *Photosynth. Res.* **1995**, *46*, 177–184.
- (9) Blomberg, M. R. A.; Siegbahn, P. E. M.; Styring, S.; Babcock, G. T.; Åkermark, B.; Korall, P. *J. Am. Chem. Soc.* **1997**, *119*, 8285–8292.
- (10) Caudle, M. T.; Pecoraro, V. L. *J. Am. Chem. Soc.* **1997**, *119*, 3415–3416.
- (11) Tommos, C.; Babcock, G. T. *Acc. Chem. Res.* **1998**, *31*, 18–25.
- (12) Gupta, R.; MacBeth, C. E.; Young, V. G.; Borokik, A. S. *J. Am. Chem. Soc.* **2002**, *124*, 1136–1137.
- (13) Baldwin, M.; Pecoraro, V. L. *J. Am. Chem. Soc.* **1996**, *118*, 11325–11326.
- (14) Wang, K.; Mayer, J. *J. Am. Chem. Soc.* **1997**, *119*, 1470–1471.
- (15) Rüttiger, W.; Campana, C.; Dismukes, G. C. *J. Am. Chem. Soc.* **1997**, *119*, 6670–6671.
- (16) Ruettinger, W. F.; Dismukes, G. C. *Inorg. Chem.* **2000**, *39*, 1021–1027, 4186 (correction).

- (17) Carrell, T. G.; Cohen, S.; Dismukes, G. C. *J. Mol. Catal. A: Chem.* **2002**, *187*, 3–15.

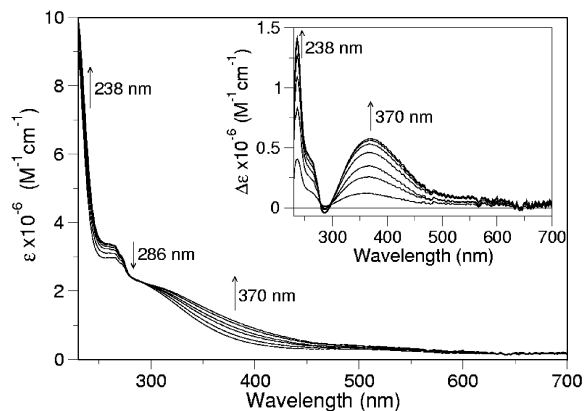
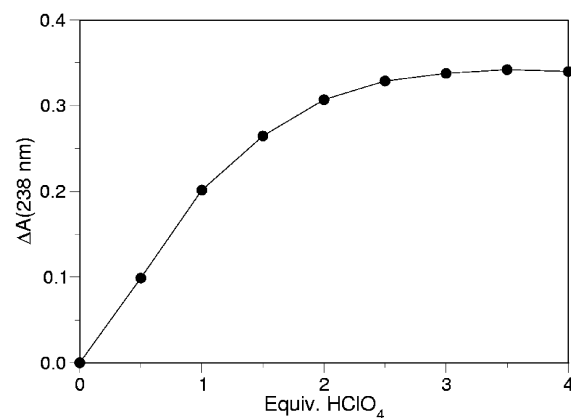
Scheme 1. Absorbance Spectra of PzH, PzH⁺•, pz•, and pz⁺ in CH₂Cl₂ and Selected Band Peaks

The UV-vis spectrum of the resulting solution of **1H** shows no trace of pzh or any of its oxidized derivatives.

Synthesis of Phenothiazine Derivatives. pzh⁺(ClO₄⁻) was prepared using the method of Billon¹⁸ and confirmed by its characteristic UV-vis absorption (Scheme 1). The unique EPR spectra of pz• and pzh⁺ were used to confirm these species.¹⁶ Synthesis of pz⁺(ClO₄⁻) was performed by stoichiometric reaction between **1**⁺ and pzh. pzh (7 mg) in 10 mL of CH₂Cl₂ was added dropwise to 60 mg of **1**⁺(ClO₄⁻) dissolved in 10 mL of CH₂Cl₂. The mixture was stirred for 3 h. A purple precipitate of pz⁺(ClO₄⁻) appears and was filtered and washed twice with 5 mL of CH₂Cl₂. This solid exhibits UV-vis, FTIR, and NMR spectra that match those of pz⁺(ClO₄⁻) prepared by a literature method (Supporting Information).¹⁸ Notably, the FTIR spectrum of pz⁺(ClO₄⁻) is devoid of the peaks characteristic of the Ph₂PO₂⁻ ligand, indicating no loss of phosphinate from **1**⁺(ClO₄⁻). The pz• neutral radical was prepared in solution by deprotonation of the pzh⁺ radical cation with 1 equiv of triethylamine (10 μL of a 5 mM solution of Et₃N in CH₂Cl₂ was added to 2 mL of a 0.025 mM solution of **1**⁺ in the same solvent). The radical decays over tens of minutes, so that it was prepared immediately prior to use.

Results and Discussion

Synthesis of [Mn₄O₄(O₂PPh₂)₆]⁺(ClO₄⁻), **1⁺(ClO₄⁻).** Previously, we reported that **1** can be quantitatively oxidized to **1**⁺ in nonaqueous solution either electrochemically (E°

**Figure 1.** Titration of HClO₄ into a 0.10 mM solution of **1** in CH₂Cl₂ at 20–25 °C monitored by UV-vis spectrophotometry. Inset: Difference spectra relative to the initial spectrum of **1**.**Figure 2.** Change in absorbance at 238 nm as HClO₄ is added to a 0.10 mM solution of **1**.

= 1.4 V vs NHE)¹⁵ or by oxidation with O₂ following addition of anhydrous triflic acid (HOTf) or anhydrous (Me₃-Si)OTf (OTf⁻ = trifluoromethanesulfonate, CF₃SO₃⁻), forming [Mn₄O₄(O₂PPh₂)₆]OTf (**1**⁺(OTf⁻)) in near quantitative yield.¹⁹ This material was extensively characterized both spectroscopically (UV-vis, ¹H NMR, EPR, FTIR, ESI-MS) and crystallographically (XRD). Here, we extend this chemistry to show that oxidation of **1** in aqueous perchloric acid (HClO₄) produces **1**⁺(ClO₄⁻) under simpler conditions without the need for anhydrous conditions.

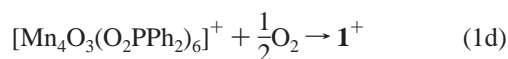
UV-vis spectrophotometry in Figure 1 reveals the conversion of the red-brown solution of **1** in air-saturated CH₂Cl₂ to a brown solution of **1**⁺ upon addition of HClO₄. Positive peaks are observed in the difference spectra at 238 and 370 nm with shoulders at 260 and 570 nm, as well as a negative peak centered at 286 nm (Figure 1, inset). Two isosbestic points are observed at 275 and 300 nm, consistent with the simple conversion between two species. The change in absorbance of the band at 238 nm was used to determine the end point of the reaction, which is seen to be complete at 2 equiv of HClO₄ (Figure 2); no further reaction is observed in excess HClO₄. This same end point is observed at 370 nm (not shown). The UV-vis spectra from the

(18) Billon, J.-P. *Ann. Chim. (Paris)* **1962**, *7*, 190–196.(19) Ruettinger, W. F.; Ho, D. M.; Dismukes, G. C. *Inorganic Chemistry* **1999**, *38*, 1036–1037.

previously characterized reactions of HOTf and (Me₃Si)OTf with **1**¹⁹ are identical to those observed in the reaction of HClO₄ with **1** and also reveal an endpoint at approximately 2 equiv of HOTf or (Me₃Si)OTf.

The product from this reaction, **1**⁺(ClO₄⁻), was isolated as a pure solid as described in the Experimental Section. The ¹H NMR spectrum of **1**⁺(ClO₄⁻) dissolved in CD₂Cl₂ shows two broad peaks at 6.8 and 8.2 ppm distinct from the starting material (**1**) and match those previously reported for **1**⁺(OTf⁻).¹⁹ The spectrum is thus independent of the identity of the counteranion and free of unreacted **1** (Supporting Information). The FTIR spectrum of the product (measured in KBr) gives the same cation peaks with differences attributable to the expected replacement of OTf⁻ by ClO₄⁻ (Supporting Information). A characteristic feature of the spectra of both **1**⁺(OTf⁻) and **1**⁺(ClO₄⁻) is the band arising from the symmetric O–P–O stretch at 967 cm⁻¹, which is shifted from 989 cm⁻¹ in **1** and does not depend on the counteranion. Additionally, the peak at 633 cm⁻¹ in **1**, that has been assigned to a Mn–O stretch based on ¹⁸O-isotopic labeling, is shifted to 624 cm⁻¹ in the ClO₄⁻ oxidation product but is shifted to 638 cm⁻¹ in the OTf⁻ product. The EPR spectrum of **1**⁺ measured at 4–10 K was previously reported and assigned to the zero-field splitting of an *S* = 5/2 ground state.²⁰ The positive-ion ESI-MS spectrum of **1**⁺(ClO₄⁻) is identical to that previously reported for **1**⁺(OTf⁻) dissolved in CH₂Cl₂, with only a single peak appearing at *m/z* 1586 attributable to the mass of the parent ion **1**⁺ (not shown). All available spectroscopic data thus indicate that strong acids enable the quantitative oxidation of **1** by O₂ to form [Mn₄O₄(O₂PPh₂)₆]⁺X⁻, X⁻ = ClO₄⁻ or OTf⁻.

The intermediates seen in the oxidation of **1** to **1**⁺ indicate a two-step pathway (eq 1).¹⁹ Fifty percent of the final yield of **1**⁺ forms initially under anaerobic conditions upon outersphere oxidation of **1** by the protonated precursor **1H**⁺ (eq 1a,b). The remaining 50% yield of **1**⁺ forms by steps 1c and d in the presence of O₂ upon protonation of intermediate **1H** (formed in step b) to produce [Mn₄O₃(O₂PPh₂)₆]⁺ by loss of a corner hydroxo as water molecule. The latter species is seen as the major intermediate by ESI-MS in the formation of **1**⁺ from O₂.



Proton-Coupled Electron Transfer Reactions of **1⁺(ClO₄⁻).** Phenthiazine (pzH) is an aromatic amine that is capable of performing redox reactions involving the

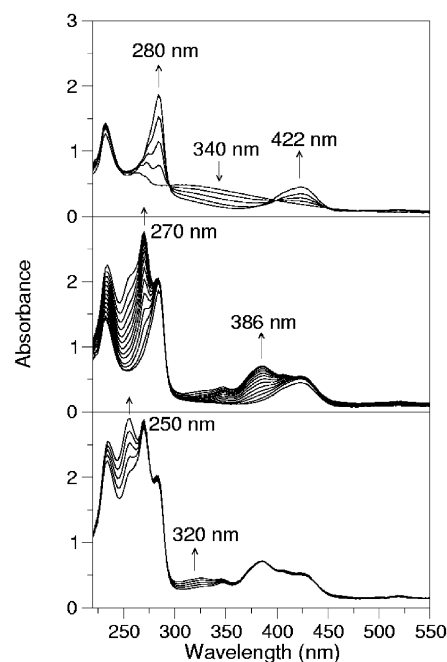


Figure 3. Titration of pzH into a 0.025 mM solution of **1**⁺(ClO₄⁻) monitored by UV–vis spectrophotometry in CH₂Cl₂ solvent at 20–25 °C. Top: 0–1 equiv of pzH. Middle: 1–4 equiv of pzH. Bottom: 4–5 equiv of pzH.

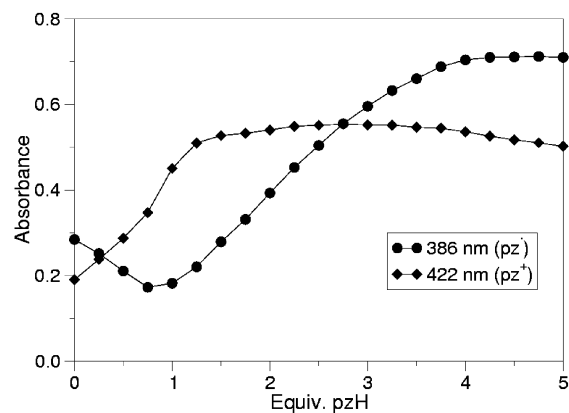


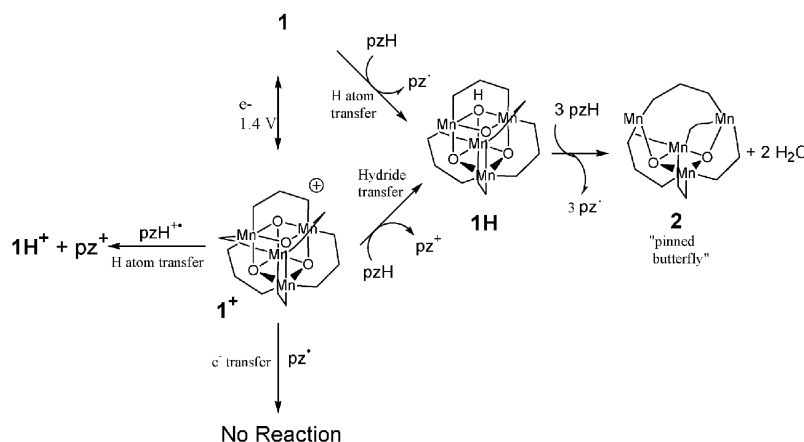
Figure 4. Change in absorbance at wavelengths that represent the concentration of oxidized phenothiazine species during the titration of pzH into **1**⁺(ClO₄⁻). Legend: ● 386 nm (pz*), ◆ 422 nm (pz⁺).

transfer of either one or two electrons, either coupled to the removal of the proton or not. Each of the possible oxidized species (pzH^{•+}, pz*, and pz⁺) exhibits a distinctive UV–vis spectrum of known absorptivity that permits unambiguous identification and stoichiometry determination (Scheme 1).¹⁸ Identification of pzH^{•+} and pz* was also deduced by EPR spectroscopy based on their distinctive ¹H hyperfine structure.¹⁶

The equilibrium absorption spectral changes produced during the reaction of 1–5 equiv pzH with **1**⁺(ClO₄⁻) (Figure 3) can be broken down into three distinct phases. These are most clearly seen by examining the absorbance changes at 386 nm (corresponding to a maximum for pz*; Scheme 1) and 422 nm (corresponding to a maximum for pz⁺ and a shoulder of pz*) as shown in Figure 4. Phase I, from 0 to 1 equiv of added pzH (Figure 3 (top), Figure 4), shows the appearance of a sharp band centered at 280 nm, as well as

(20) Aromí, G.; Aubin, S. M. J.; Bolcar, M. A.; Christou, G.; Eppley, H. J.; Foltling, K.; Hendrickson, D. N.; Huffman, J. C.; Squire, R. C.; Tsai, H.-L.; Wang, S.; Wemple, M. W. *Polyhedron* **1998**, *17*, 3005–3020.

Scheme 2



a broader band at 422 nm, consistent with the appearance of pz^+ , arising from the removal of hydride from pzH . Two isosbestic points are observed during this phase at 300 and 400 nm.

Phase II, from 1 to 4 equiv of pzH (Figure 3 (middle), Figure 4), shows new bands at 270, 350, and 386 nm, consistent with the appearance of pz^+ , arising from the removal of a hydrogen atom from pzH . The absorbance of the band at 422 nm does not change during this phase, indicating that pz^+ formed in phase II arises exclusively from pzH , and not from reactions involving pz^+ formed during phase I.

Phase III, from 4 to 5 equiv of pzH (Figure 3 (bottom), Figure 4), shows new bands at 250 and 320 nm, consistent with the spectrum of pzH . The intensities of the bands that appeared in phases I and II are unchanged during phase III. These changes indicate that no further reaction occurs following the addition of 4 equiv of pzH . Scheme 2 summarizes the $pzet$ reactions of $1^+(ClO_4^-)$ with 1–4 equiv of pzH based on these absorption data and corroborated by spectroscopic characterizations of the Mn products, as described next.

Solution Structure of $1H$. The hydride transfer product between 1^+ and the first equivalent of pzH was isolated and found to be $Mn_4O_3(OH)(O_2PPh_2)_6$ ($1H$). This molecule contains the $[Mn_4O_3(OH)]^{6+}$ core, which is a known core type, having been previously identified in the complex $Mn_4O_3(OH)(O_2CMe)_3(dbm)_3$ with mixed ligands (carboxylato/dibenzoylmethane).²⁰ Crystallization trials of $1H$ resulted in a microcrystalline product that did not diffract well enough for XRD analysis. Poor diffraction has been observed with other partially reduced cubane products prepared with the Ph_2PO_2H ligand and is a common outcome of the high symmetry of this approximately tetrahedral molecule which leads to disorder in the lattice. Therefore, spectroscopic analyses by EPR, 1H NMR, FTIR, ESI-MS, and LDI-MS were performed to determine the composition, oxidation state, and magnetic properties, as described next.

The absorbance spectrum of $1H$ dissolved in CH_2Cl_2 is unique compared to the spectra of both 1 and 1^+ (Figure 5). Characteristic peaks at 240 nm ($\epsilon = 37\,000\ M^{-1}\ cm^{-1}$) and 270 nm ($\epsilon = 25\,000\ M^{-1}\ cm^{-1}$) are associated with

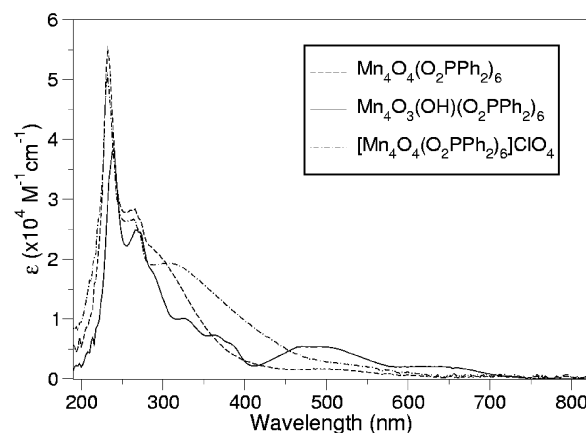


Figure 5. Electronic absorption spectra of $1H$ (in CH_3CN), 1 (in CH_2Cl_2), and $1^+(ClO_4^-)$ (in CH_2Cl_2) plotted at equal molar concentrations.

transitions within the diphenylphosphinate ligand, while seven other bands at 287 nm (shoulder), 326 nm ($\epsilon = 10\,000\ M^{-1}\ cm^{-1}$), 362 nm ($\epsilon = 7400\ M^{-1}\ cm^{-1}$), 382 nm (shoulder), 490 nm ($\epsilon = 5500\ M^{-1}\ cm^{-1}$), 510 nm ($\epsilon = 5400\ M^{-1}\ cm^{-1}$), and 645 nm ($\epsilon = 2100\ M^{-1}\ cm^{-1}$) involve transitions within the $[Mn_4O_3(OH)]^{6+}$ core or between the core and the phosphinate ligands of $1H$. The latter bands are seen to be more dispersed in energy, shifted to lower energy and greater in number than are resolved in the spectrum of 1 . These features indicate that the $[Mn_4O_3(OH)]^{6+}$ core in $1H$ has lower symmetry and lower energy excited states than the tetrahedral $Mn_4O_6^{6+}$ core in 1 .

The room temperature 1H NMR spectrum of $1H$ in acetone- d_6 exhibits a number of broad poorly resolved peaks at 3.6, 5.0, 6.6, 7.0, 7.4, 8.8, 9.6, 9.8, 10.6, and 14.0 ppm (Figure 6). Because of the broad, unresolved nature of the spectrum, peak assignments are not possible. The broadening suggests a paramagnetic state, as is expected based on the electron count and is confirmed by EPR studies (described later). The large number of peaks indicates a lower symmetry cluster relative to both 1 and 1^+ , for which all six $Ph_2PO_2^-$ ligands are equivalent by 1H NMR in CD_2Cl_2 solution at room temperature.^{15,19} A few sharp peaks are observed between 7.6 and 8.6 ppm that represent a minor fraction of the integrated spectral area. These peaks are due to free phosphinate (or phosphinic acid) which reflects partial ligand

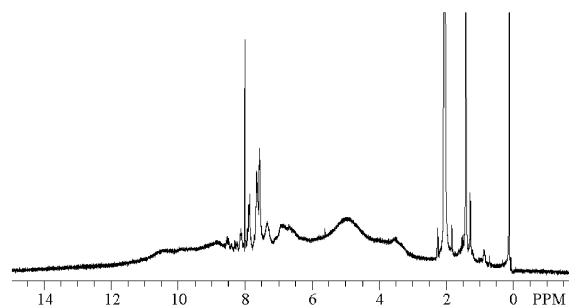


Figure 6. ^1H NMR spectrum of **1H** in CD_2Cl_2 at $20\text{--}25\text{ }^\circ\text{C}$.

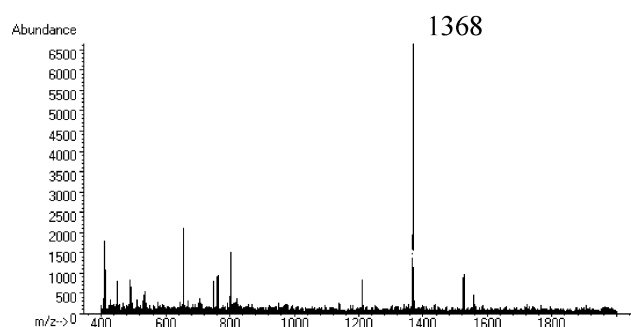


Figure 7. Positive-ion electrospray ionization mass spectrum of a solution of **1H** in acetone.

dissociation of **1H** in acetone. Sharp peaks below 2.2 ppm are from the solvent.

The FTIR spectrum of **1H** exhibits many of the general characteristics displayed by **1** and **1⁺** (Supporting Information). A band at 624 cm^{-1} (medium strength) is tentatively assigned to a $\text{Mn}\text{--}\text{O}$ core stretching mode by analogy to a similar band observed in **1** and **1⁺** at 633 and 624 cm^{-1} , respectively, assigned on the basis of $^{18}\text{O}/^{16}\text{O}$ isotopic shift.^{15,19} A strong band at 993 cm^{-1} is also tentatively assigned to the symmetric $\text{O}\text{--}\text{P}\text{--}\text{O}$ stretch, also by analogy to the spectra of **1** and **1⁺** where it is observed at 989 and 967 cm^{-1} , respectively.

EPR spectroscopy of **1H** was examined at 9.5 GHz over the temperature range $3.7\text{--}50\text{ K}$ (Supporting Information). A broad isotropic signal at $g = 2.006$ lacking hyperfine structure is observed. These data, together with a Curie temperature dependence from 3.7 to 15 K , support the assignment of a paramagnetic ground state of unknown spin.

The positive-ion electrospray ionization mass spectrum of **1H** in a solution of acetone (Figure 7) exhibits a major peak with $m/z = 1368$ which corresponds to the mass of the ion $[\text{Mn}_4\text{O}_4(\text{O}_2\text{PPh}_2)_5]^+$ formed by removal of $\text{Ph}_2\text{PO}_2\text{H}$ from **1H**. The parent ion of **1H** at $m/z = 1587$ is not observed in the ESI mass spectrum. This result indicates the lability of one Ph_2PO_2^- ligand from **1H** under the ESI conditions and is consistent with low level dissociation of phosphinate from **1H** also seen in acetone by NMR (Figure 6). The phosphinate ligand dissociation chemistry of **1H** in solution is reminiscent of the behavior of $\text{Mn}_4\text{O}_2(\text{O}_2\text{PPh}_2)_6$, **2**.¹⁶ Selective dissociation of one Ph_2PO_2^- ligand from **2** occurs under the ESI detection conditions to produce $[\text{Mn}_4\text{O}_2(\text{O}_2\text{PPh}_2)_5]^+$ ($m/z = 1337$). We conclude that the products of reduction of **1⁺** to

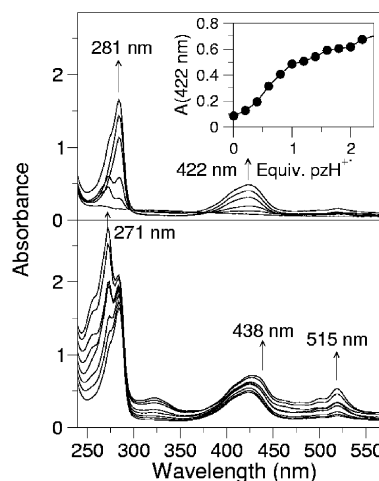


Figure 8. Titration of $\text{pzH}^+(\text{ClO}_4^-)$ into a 0.025 mM solution of **1⁺**(ClO_4^-) monitored by UV-vis spectrophotometry. Top: $0\text{--}1$ equiv of $\text{pzH}^+(\text{ClO}_4^-)$. Bottom: $1\text{--}2$ equiv of $\text{pzH}^+(\text{ClO}_4^-)$.

1H and to **2** are complexes having enhanced lability of one phosphinate ligand in solution compared to their oxidized precursors.

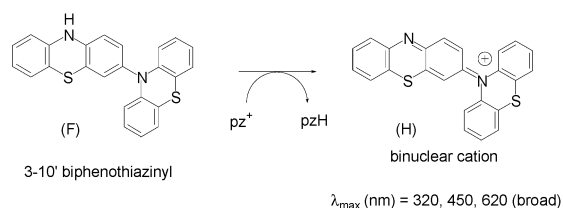
Proton-Coupled Electron Transfer Reaction of the pzH^+ Cation Radical with **1⁺(ClO_4^-).** The reaction of the phenothiazine radical cation pzH^+ with **1⁺**(ClO_4^-) was investigated by UV-vis titration (Figure 8). In this reaction, 1 equiv of $\text{pzH}^+(\text{ClO}_4^-)$ reacts with **1⁺**(ClO_4^-) to produce the pz^+ cation via a net hydrogen atom transfer. Formation of the pz^+ cation was confirmed by the appearance of bands exclusively at 281 and 422 nm and the absence of bands for the pz^* radical. Stoichiometry requires that the protonated cubane **1H⁺** should be the product. However, we could not confirm this directly since the pz^+ and **1H⁺** products were not readily separable, nor is the UV-vis spectrum of the manganese product sufficiently intense in the reaction mixture owing to overlap with the much stronger bands from pz^+ . No reaction occurs upon the subsequent addition of excess pzH^+ cation radical, as confirmed by the appearance of bands at 271 , 438 , 480 , 499 , and 515 nm for unreacted pzH^+ . Hence, only the first equivalent of pzH^+ reacts with **1⁺**, and this reaction is inferred to be H atom transfer on the basis of the pz^+ product.

Additionally, there is a much slower reaction that occurs over tens of minutes that produces bands at 250 , 320 , 470 , and 620 (broad), while the bands for pzH^+ and pz^+ disappear simultaneously (not shown). The products of this slow reaction were not further investigated, except to note that pzH^+ was previously shown by Hanson and Norman²¹ to form the dimer 3-10'-biphenothiazinyl in solution (**F**) which is oxidized by the pz^+ cation to form the binuclear cation (**H**) (Scheme 3). The latter species was shown to absorb at 320 , 450 , and 620 nm , while the bands for pzH (formed by reduction of pz^+) appear at 256 and 320 nm .²² Our absorbance data indicate that the same slow reaction occurs as reported by these authors.

(21) Hanson, P.; Norman, R. O. C. *J. Chem. Soc., Perkin II* **1973**, 264.

(22) (We are indebted to a reviewer for bringing this chemistry to our attention.)

Scheme 3



Absence of Reaction between the pz^{\bullet} Neutral Radical and $1^+(\text{ClO}_4^-)$. The addition of 1 equiv of the neutral pz^{\bullet} radical to $1^+(\text{ClO}_4^-)$ in CH_2Cl_2 is shown in Figure 9. The resulting spectrum is equivalent to the addition spectrum of 1^+ and the neutral pz^{\bullet} radical, indicating that no reaction occurs on a time scale less than 5 min. Importantly, spectral bands near 419 and 281 nm for the pz^+ cation are not observed, indicating that electron transfer to form **1** does not occur. Spectral changes that correspond to dismutation of the pz^{\bullet} radical occur at longer times (not shown).

Scheme 2 summarizes the reactions of 1^+ with pzH (1–4 equiv), the cation radical $pzH^{\bullet+}$, and the neutral pz^{\bullet} radical. The data reveal that proton-coupled electron transfer reactions are the only reactions that occur, leading to hydride and hydrogen atom transfer, from pzH and $pzH^{\bullet+}$, respectively, with no evidence for electron transfer from pzH or the pz^{\bullet} radical.

Oxidation of Phenols by **1.** The reaction of a series of *p*-substituted phenols (*p*-Me, Ph, ^tBu, Br, and CN) with **1** was investigated by UV–vis absorbance changes in order to access the dependence of the stoichiometry of the initial H atom transfer reaction on the O–H bond energy. Uniform bleaching of the absorbance from **1** was observed at all wavelengths above 300 nm when the phenol was used in excess, while bands due to **1H** were discerned as an intermediate with less than 1 equiv of phenol. In the reaction with phenol, the visible bands from **1** are bleached and replaced by bands with peaks at 400 and 550 nm and isosbestic points at 380 and 430 nm due to formation of 4,4'-biphenylquinone (Figure 10). This is the expected carbon radical coupling product for the phenoxyl radical precursor. The *para*-substituted phenols all produced bleaching of the absorbance from **1**, although at different rates and, as expected, without formation of the bands due to the carbon radical coupling product (not shown). The initial step for all of the phenols involves H atom transfer to yield the corresponding phenoxyl radical and **1H**.

Formation of the Reduced “Pinned Butterfly” $Mn_4O_2(O_2PPh_2)_6$ (2**).** The stoichiometry of the overall reaction of pzH with $1^+(\text{ClO}_4^-)$, as determined from the molar absorptivities of the oxidized phenothiazine products, is given in Scheme 2 and compared to the previously characterized reaction of pzH with **1**.¹⁶ In the latter reaction, 4 equiv of pzH reduces **1** by transferring four electrons and four protons, resulting in the release of two of the μ_3 -oxo ligands as H_2O molecules and forming $Mn_4O_2(O_2PPh_2)_6$ (**2**).

Since 1^+ is simply one electron higher in oxidation state than **1** with no major core structural change in the solid-state other than trigonal distortion,¹⁹ the equivalence of the

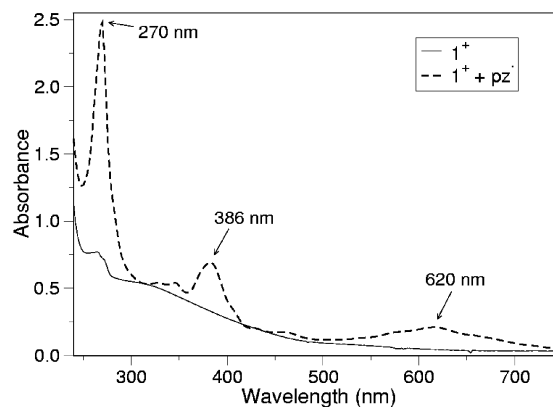


Figure 9. Solid line: UV–vis spectrum of $1^+(\text{ClO}_4^-)$ in CH_2Cl_2 . Dashed line: Spectrum that results from the addition of 1 equiv of the pz^{\bullet} radical to a CH_2Cl_2 solution of $1^+(\text{ClO}_4^-)$.

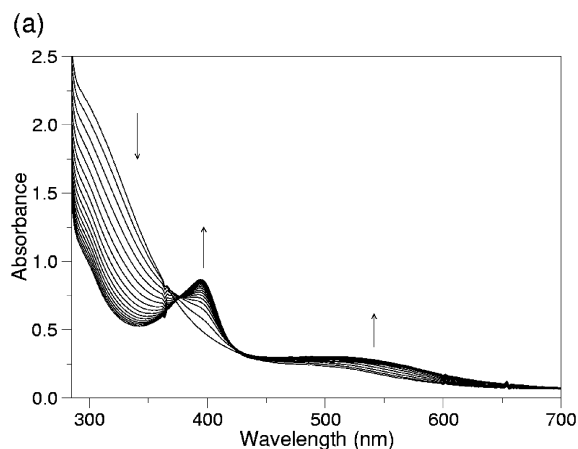


Figure 10. Absorbance changes observed during the reaction of phenol with **1**. Conditions: $[1] = 0.10 \text{ mM}$ in CH_2Cl_2 ; $[\text{phenol}] = 3.0 \text{ mM}$; spectra were collected in 60 s intervals.

stoichiometries of the overall reactions of pzH with 1^+ and with **1** indicates that the manganese product **2** should be the same. Complex **2** has been formulated as $Mn_4O_2(O_2PPh_2)_6$ on the basis of solution phase UV–vis, ESI-MS of the ¹⁸O/¹⁶O-isotopomers, ¹H NMR, FTIR, and EPR data.¹⁶ These data support a structure in which all six phosphinate ligands remain bound to the $Mn_4O_2^{6+}$ core, most probably facially bridging between the Mn ions to create a “pinned butterfly” core type. The formation of complex **2** in the reaction of pzH with 1^+ was confirmed using UV–vis and FTIR spectroscopies in CH_2Cl_2 solution. FTIR bands in 400–650 cm^{-1} and 950–1200 cm^{-1} ranges contain many of the characteristic peaks of **1** and 1^+ and are not obscured by solvent bands. The reaction of four pzH with **1** to produce **2** is characterized by bands at 537, 565, 997, 1024, 1050, 1131, and 1161 cm^{-1} in the solution FTIR spectrum (Supporting Information). All of these bands, as well as an additional band at 1086 cm^{-1} which is a characteristic band of ClO_4^- , are observed following the reaction of four pzH with 1^+ (Supporting Information). Additionally, a broad peak is observed in the far-IR range at 3600 cm^{-1} following the addition of 4 equiv of pzH to 1^+ (Supporting Information). This peak appears between 2 and 4 equiv pzH and was previously assigned to water produced by reduction of the cluster.¹⁶ This assignment was confirmed on the basis of the

H/D isotope shift and reference spectra for D₂O/H₂O in dichloromethane.

Attempts to isolate **2** from solution were unsuccessful as it is unstable upon concentrating, which leads to precipitation of an insoluble polymeric species [Mn^{II}(O₂PPh₂)₂]_∞ (**3**).¹⁶ This reaction occurs slowly over hours in CH₂Cl₂ solution or more rapidly upon removal of solvent. Stripping the solvent from a reaction mixture containing **1**⁺ and 4 equiv of pzH produces a tan solid that is insoluble in all common solvents. The FTIR spectrum of this resulting solid indicates that it is identical to compound **3**, formed by precipitation of the product of the reaction of **1** with 4 equiv of pzH (Supporting Information). The FTIR spectrum of this material closely matches that of polymeric Mn(O₂PPh₂)₂(pyridine)₂.¹⁶ Polymerization of **2** is to be expected considering the low coordination number of the wingtip Mn(II) ions in the Mn₄O₂⁶⁺ core and the lability of one of the phosphinate ligands observed during ionization by ESI-MS.

Conclusions

The reduction chemistry of the all-oxo manganese cubanes has been extended to include the five-electron four-proton reduction of **1**⁺ by pzH to form the “pinned-butterfly” complex **2** and two water molecules. The overall stoichiometry is the same as is observed in the reduction of **1** by pzH (Scheme 2). However, the first equivalent of pzH reacts by hydride transfer to **1**⁺, whereas hydrogen atom transfer is observed in the reaction with **1**.

In contrast to the pcat reactions of **1** and **1**⁺ with pzH derivatives, electron-only reductants such as cobaltocene or stronger reductants such as formate completely reduce both **1** and **1**⁺ to free Mn(II) and cause cluster fragmentation.¹⁵ No stable intermediates are seen with cobaltocene, while formate produces partially reduced states of the cluster similar to pzH. But unlike pzH, when used in excess of 4 equiv formate fully reduces the cluster to the all Mn(II) level and causes fragmentation of the core according to ESI-MS results (I. Kaneko, unpublished results). The X–H bond dissociation energies for these reactions provide a thermodynamic basis for these observations, as discussed next.

The O–H bond dissociation enthalpy (BDE) of **1H** was estimated using a thermodynamic cycle where H[•] is transferred from another species (HA = pzH, etc.) as in eq 2.^{3,23} The standard free energy Δ*G*[°] is calculated (eq 3) from the known *E*[°] and *K*_a values and is taken to be approximately equal to the Δ*H*[°] assuming Δ*S*[°] ≈ 0. The derived Δ*H*[°] is the difference between the H–O(**1**) and H–A bond strengths in solution. The derived solution H–A bond strengths can be compared to gas phase values (when available) to judge whether the assumption of zero differential solvation of HA and A is justified. In the case of arylamines such as phenylamine, the gas phase and DMSO solution phase BDEs are identical.^{24,25} This approach gives an N–H BDE of 87.1 kcal/mol for pzH in DMSO.²⁴ In the case of the phenols, the O–H BDE was estimated by this method to be Ph(87.7)

< Me(89) ~ ^tBu(89) < H(90) < Br(90.9) < CN(94.4) in DMSO or about 3–5 kcal/mol higher than in the gas phase.²⁶ Since in all of these cases the substituted phenols were oxidized by **1** to give **1H**, we can place a lower limit for the O–H BDE for **1H** to be greater than 94.4 kcal/mol.



$$\Delta H^{\circ} = \text{BDE}(\text{H}-\text{A}) - \text{BDE}(\text{H}-\text{O}(\mathbf{1})) = 23.06[E^{\circ}(\text{A}^{\bullet}) - E^{\circ}(\mathbf{1})] + 1.37[\text{p}K_{\text{a}}(\text{HA}) - \text{p}K_{\text{a}}(\mathbf{1H})] \quad (3)$$

Parker has used a similar thermodynamic cycle to directly compute BDEs by reference to standard redox potentials in a common solvent.²⁷ Unfortunately, the lack of solubility of **1** in common solvents makes estimates based on this method more unreliable. Thus, the reduction potential of **1** was previously reported to be –0.09 V in CH₂Cl₂, the only pure solvent for which data are available. The p*K*_a of phenothiazine (p*K*_a = 22.6 in DMSO or water)²⁴ was used to set a lower limit for the p*K*_a of **1H**, based on our observation that the pz[–] anion (the conjugate base of pzH) does not remove a proton from **1H** in CH₂Cl₂ or mixed CH₂Cl₂/MeCN solvent. The p*K*_a may be considerably higher, but it is not easy to find a suitable range of strong bases to determine this value more precisely that are not also oxidized by **1H**. This lower limit for the p*K*_a reinforces the previous comparisons with substituted phenols, showing that the O–H BDE of **1H** must be higher than 94.4 kcal/mol.

With a BDE in excess of 94.4 kcal/mol, **1H** appears to have one of the stronger O–H bonds of any reported aquo or hydroxo ligand bound to a complex of Mn^{III}, Mn^{IV}, or Mn^{VII} reported thus far, and it is less than 25 kcal/mol weaker than the BDE for gas phase water (119 kcal/mol). For example, it is greater than the free energy for cleavage of the O–H bond from a terminal water ligand in a series of Mn^{III}₂L₂ OH₂ and Mn^{IV}₂L₂ OH₂ complexes (BDE = 82–94 kcal/mol),¹⁰ as well as the bridging μ₂-hydroxo ligand in Mn^{III}Mn^{IV} complexes (BDE = 77 kcal/mol).^{13,14} These all possess six-coordinate Mn ions. It may be compared to the strongest O–H bond observed thus far (BDE = 110 kcal/mol) for a terminally coordinated hydroxide ligand in a mononuclear Mn^{III}(OH)polyamido complex possessing trigonal bipyramidal coordination.¹² Density functional calculations also reveal a large O–H BDE in a neutral monomeric complex of Mn^{III}O–H upon conversion to Mn^{IV}=O by formal transfer of a hydrogen atom (BDE = 103 kcal/mol).²⁸

These comparisons reveal that the [Mn₄O₃OH]⁶⁺ core in **1H** activates the O–H bond for cleavage to a lesser extent than do the rhombohedral dimanganese cores in [Mn₂(OH)₂]⁵⁺ and Mn₂O(OH)⁴⁺ compounds. This difference could have been anticipated based on structural data showing

(24) Bordwell, F. G.; Zhang, X.-M.; Cheng, J.-P. *J. Org. Chem.* **1993**, *58*, 6410–6416.

(25) Varlamov, V.; Demisov, E. *Chem. Abstr.* **1988**, *108*, 130931p; **1987**, *293*, 126–128.

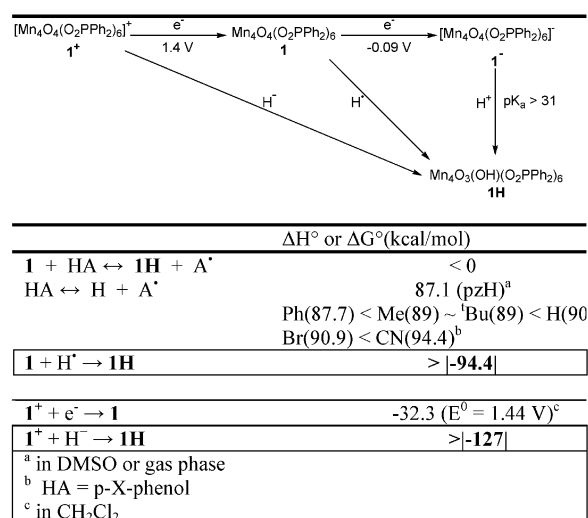
(26) Bordwell, F. G.; Cheng, J.-P. *J. Am. Chem. Soc.* **1991**, *113*, 1736–1743.

(27) Parker, V. D. *J. Am. Chem. Soc.* **1991**, *114*, 7458–7462.

(28) Blomberg, M. R. A.; Siegbahn, P. E. M. *Theor. Chem. Acc.* **1997**, *97*, 72–80.

(23) Bordwell, F. G.; Cheng, J.-P.; Ji, G.-Z.; Satish, A. V.; Zhang, X. J. *Am. Chem. Soc.* **1991**, *113*, 9790–9795.

Scheme 4



that **1** contains an expanded core with relatively longer and thus weaker Mn–O bonds than those observed in the $Mn_2O_2^{3+}$ core,^{15,29} and also by the comparatively larger pK_a of **1H** ($pK_a > 22.6$).¹⁰ The strong O–H bond in **1H** also rationalizes the oxidation chemistry of **1** which has been shown to catalyze the oxidation of toluene, alkanes, alkenes, phosphines, and sulfides by *t*-butylhydroperoxide.¹⁷ Two reaction pathways were identified with different substrates: either a two-electron pathway via a putative Mn(V)=O intermediate or a one-electron pathway via hydrogen atom abstraction.

The affinity of I^+ for the hydride ion can be estimated by extending the thermochemical cycle in Scheme 4 to include the reduction potential for I/I^+ . This method has been developed by Parker and co-workers for solution phase reactions³⁰ and applied to manganese complexes by Mayer.^{3,31} Using the lower limit for the BDE of **1H** in CH_2Cl_2 and the reduction couple for I^+/I (1.44 ± 0.04) in CH_2Cl_2 , the free energy for the dissociation of hydride from **1H** is estimated to be greater than 127 kcal/mol. This value may be compared to the heterolytic bond dissociation free energy of 122 kcal/mol for hydride abstraction from $[L_2Mn(\mu-O)-(\mu-OH)MnL_2]^{3+}$, $L = 1,10$ phenanthroline.³² The latter molecule is produced by hydride abstraction from substituted toluenes by $[L_2Mn(\mu-O)_2MnL_2]^{4+}$. This novel reaction is a rare example of hydride abstraction by metal-mediated hydrocarbon oxidation. For example, it contrasts with the strong preference for hydrogen atom abstraction by numerous metal- or radical-oxidants, including permanganate (MnO_4^-).^{3,12,31} Accordingly, we can anticipate that future reactivity studies of I^+ may reveal it to be a potent oxidant for the oxidation of hydrocarbons via hydride abstraction.

These large heterolytic and homolytic bond dissociation energies for **1H** provide a thermodynamic basis for the

reactions given in Scheme 2. Complex I^+ abstracts hydride from pzH because the driving force for reaction is roughly 32 kcal/mol greater than that of hydrogen atom transfer. On the other hand, **1** abstracts a hydrogen atom from pzH rather than a hydride because pzH has a weaker N–H bond (87.1 kcal/mol)²⁴ than does **1H**. Both reactions involve formation of neutral products which are strongly favored over ionic products in nonpolar solvent and by the nonpolar phenyl groups of the diphenylphosphinate ligands. Similarly, the absence of oxidation of the pz[•] radical by I^+ via simple electron transfer to form the pz⁺ cation (Scheme 2) can also be explained based on electrochemical data showing that oxidation of the pz[•] radical by I^+ is unfavorable by 0.2 V. The reduction potential for the I^+/I couple was previously found to be +0.680 V versus ferrocene (Fc) in CH_2Cl_2 (converted to 1.4 V vs NHE),¹⁵ while the electrode potential for the pz^{+/pz[•]} couple was measured by cyclic voltammetry and yielded the value 0.860 V versus Fc in CH_2Cl_2 (courtesy of Dr. M. Yagi) comparable with earlier works in other solvents.³³

The Mn_4O_4 -cubane topology has been conjectured as a possible structural model for the photosynthetic Mn_4O_x core in its highest oxidation state (“ S_4^+ ”), with two of the bridging oxo sites serving as the water binding sites in the reduced form.^{34,35} Comparisons can now be made to I^+ . The O–H BDE of **1H** is considerably stronger than that observed for the O–H bond for tyrosine (BDE ~ 86 kcal/mol^{9,10}). On this basis, the triply bridging μ_3 -hydroxo found in **1H** would be energetically unsuitable as a H atom donor to the tyrosyl radical generated during turnover of the photosynthetic water oxidizing enzyme. Thus, if direct H atom transfer were to occur in the WOC enzyme, we would have to conclude that either other geometries for binding of substrate water to Mn, other Mn oxidation states, or other cofactors (Ca^{2+} ?) would have to be involved to further activate the substrate water ligand. However, emerging XRD structural data for the lower oxidation state(s) of the enzyme indicate that the tyrosine–Mn distance is too far (≥ 7.5 Å) to permit direct H atom transfer without a major structural change to reduce the distance.^{36,37} Thus, comparison of the substrate O–H bond energy difference versus tyrosine would be an inappropriate predictor of the reaction energetics and pathway, since there will then have to exist a different base to serve as the proton acceptor over such distances (pK_a change in eq 3).

The present case of net hydride transfer to I^+ provides a clear example of two-electron one-proton redox chemistry that is directly relevant to the proposed lowest-energy pathway for the oxidation of water to O_2 via a peroxo intermediate based on thermodynamic considerations, both for catalysis by the Mn_4 -cluster in the PSII-WOC,^{38,39} and

(33) Billon, J.-P. *Bull. Soc. Chim. Fr.* **1961**, 306, 1923–1929.

(34) Vincent, J. B.; Christou, G. *Inorg. Chim. Acta* **1987**, 136, L41–L43.

(35) Ruettinger, W.; Yagi, M.; Wolf, K.; Bernasek, S.; Dismukes, G. C. *J. Am. Chem. Soc.* **2000**, 122, 10353–10357.

(36) Zouni, A.; Witt, H. T.; Kern, J.; Fromme, P.; Krauss, N.; Saenger, W.; Orth, P. *Nature* **2001**, 409, 739–743.

(37) Zouni, A.; Kern, J.; Loll, B.; Fromme, P.; Witt, H.; Orth, P.; Krauss, N.; Saenger, W.; Biesiadka, J. In *PS2001 Proceedings of the 12th International Congress on Photosynthesis*; CSIRO: Melbourne, 2001.

(38) Krishtalik, L. I. *Bioelectrochem. Bioenerg.* **1990**, 23, 249–263.

(29) Manohandra, R.; Brudvig, G. W.; Crabtree, R. H. *Coord. Chem. Rev.* **1995**, 144, 1–38.

(30) Handoo, K. L.; Cheng, J.-P.; Parker, V. D. *J. Am. Chem. Soc.* **1993**, 115, 5067–5072.

(31) Gardner, K. A.; Kuehnert, L. L.; Mayer, J. M. *Inorg. Chem.* **1997**, 36, 2069–2078.

(32) Lockwood, M. A.; Wang, K.; Mayer, J. M. *J. Am. Chem. Soc.* **1999**, 121, 11894–11895.

for the uncatalyzed oxidation of free water molecules in the gas phase.⁴⁰ These calculations reveal that sequential one-electron/one-proton (hydrogen atom) transfer steps during water oxidation in both cases are thermodynamically costly and thus forbidden given the energy constraints, versus a concerted sequential two-electron/two-proton pathway via a peroxo intermediate. In the photosynthetic case, the reaction of the highest "S₄" oxidation state with water has been predicted to favor formation of a transient peroxide intermediate (unobserved) via such a two-electron/two-proton pathway.^{38,39,41} On the basis of these predictions, investigation of the chemistry of **1**⁺ with hydroxide is planned.

Mn-oxo cubanes such as **1** and other phosphinate derivatives have also been shown to undergo a unique intramolecular reaction that produces O₂ gas that is triggered by the

release of one of the bridging phosphinate ligands.³⁵ This chemistry provides a further example of the novel reactivity of this core type that has not been observed in complexes containing the [Mn₂O₂]³⁺ or [Mn₃O₆]²⁺ core.⁴²

Acknowledgment. We thank Wolfgang Ruettinger for preliminary studies, Dorothy Little for acquiring the ESI mass spectrometry data, and Masayuki Yagi for unpublished electrochemical data. This work was supported by the National Institutes of Health, Grant GM-39932. E.B. acknowledges Ecole Normale Supérieure de Lyon and the French government for financial support.

Supporting Information Available: UV-vis, ¹H NMR, and FTIR spectra (17 figures) from the reactions of HClO₄, HOTf, and (Me₃Si)OTf with **1**, the reaction of pzH with **1**⁺, and the FTIR spectra of **1H** and the isolated pz⁺(ClO₄⁻) product. This material is available free of charge via the Internet at <http://pubs.acs.org>.

IC025977E

(39) Krishtalik, L. I. *Biophysics* **1989**, *34*, 958–962.

(40) Anderson, A. B.; Albu, T. V. *J. Am. Chem. Soc.* **1999**, *121*, 11855–11863.

(41) Krishtalik, L. I. *Biophysics* **1989**, *34*, 1098–1104.

(42) Yagi, M.; Kaneko, M. *Chem. Rev.* **2001**, *101*, 21–35.